

SILICON SOLAR CELLS MADE BY  
ION IMPLANTATION AND GLOW DISCHARGE

J. P. Ponpon, P. Siffert  
Centre de Recherches Nucléaires, PREN  
F 67037 Strasbourg Cedex

**SUMMARY**

Three different methods of silicon solar cell preparation were considered and investigated: low energy ion implantation, glow discharge and prebombarded Schottky barriers. The properties of the contact layers realized by these processes are compared in terms of junction depth and sheet resistance. Preliminary results show the usefulness of these techniques for terrestrial solar cell realization.

**INTRODUCTION**

At present time most of the work devoted to silicon solar cells is concerned with diffused junctions, trying by a technology improvement to reduce the junction depth, or by using a back contact field, to increase the collection efficiency. Further studies concern the grid design and antireflective coatings. However, for terrestrial applications, new methods have to be developed in order to increase the efficiency and reduce the cost. These new methods have to be compatible with silicon ribbons or polycrystalline samples. Until now, only two other structures have been considered: implanted cells and Schottky barriers.

Ion implantation, which allows a very fine control of junction depth, doping profile and sheet resistance, was used a few years ago as a production technique having 11% AMO efficiency<sup>1</sup>. Junction depths less than 1000 Å are easily obtained by this procedure in low resistivity material, leading to a very small efficiency loss in the entrance window. As shown in fig. 1, this loss is less than 2% as long as the junction depth remains below 1000 Å. However, the cost of the sophisticated ion implantation procedure will be a definite handicap for terrestrial solar cell applications. In order to retain the advantages of ion implantation but to reduce the cost, we studied the possibility of realizing the contacts by glow discharge under correctly chosen atmospheres. The properties of these layers will be compared to those of implanted junctions.

The second process, the Schottky barrier, studied recently by ANDERSON<sup>2,3</sup> gave 8-9% AMO efficiency for chromium layers deposited on P-type silicon by vacuum evaporation. However, the efficiency of such cells depends strongly upon the barrier height  $\Phi_{B1}$  at the metal-semiconductor contact as shown in fig. 2. A process, allowing the increase of barrier height up to 1 eV is proposed. It consists of a low dose ionic bombardment prior to the Schottky barrier preparation.

**ION IMPLANTATION**

**Choice of the Implant dopant.** Several parameters have to be considered for the realization of a rectifying contact on a solar cell; the most important are a junction depth as shallow as possible and a very low sheet resistance. Ion implantation is particularly well suited to satisfy these requirements by a proper choice of the nature of the doping ion, its

energy, dose and damage-annealing treatment. Heavily doped layers, giving low sheet resistance can be obtained by ion implantation since the solubility of the group III and V dopants implanted into silicon is at least as high as that obtained when thermal diffusion is used, as reported in table I.

**TABLE I**

	Hot Implant 40 keV 450°C	Thermal diffusion 1100°C
B	2.10 <sup>20</sup>	5.10 <sup>20</sup>
Al	2.10 <sup>19</sup>	2.10 <sup>19</sup>
Ga	4.10 <sup>19</sup>	3.10 <sup>19</sup>
P	> 4.10 <sup>20</sup>	10 <sup>21</sup>
As	10 <sup>21</sup>	2.10 <sup>21</sup>
Sb	8.10 <sup>20</sup>	4.10 <sup>19</sup>
Bi	2.10 <sup>20</sup>	2.10 <sup>17</sup>

However, it must be taken into account that the electrical characteristics of an implanted layer are not determined by the number of implanted ions, but by the number of electrically active centers (dopants, defects) which is a strong function of annealing temperature. An examination of table II shows that boron is the most efficient dopant from the electrical activity point of view. We have chosen this dopant in preparing the rectifying contact on N-type silicon.

**TABLE II**

Ion Implanted Layers							
Percentage Electrically Active Ions (Identical range, 90°C annealing)							
B	Al	Ga	In	P	As	Sb	Bi
90%	10%	8%	1%	10%	20%	10%	1%

**Boron implantation into silicon.** The choice of the implant conditions results from a compromise between the three major parameters: energy, dose and annealing temperature.

**Energy:** Fig. 3 shows that the electrical activity of implanted boron after annealing is strongly energy dependent<sup>4</sup>. For example for 5 keV bombardment energy only about the half of the ion species are electrically active after high temperature annealing. Consequently, higher implant energies would be preferable in order to keep the dose lower.

But, it is clear that the thinner the implanted layer, the higher the dose necessary to reach a low sheet resistance. From fig. 1 it appears that junction depths on the order of  $1000 \text{ \AA}$  seem to be reasonable. Both our calculations and experimental determinations (fig. 4) show that this value is obtained with 10-15 keV boron ions.

**Annealing temperature:** The defects introduced by the ion bombardment can act as recombination and trapping centers for the charge carriers generated by the photons. It has been shown<sup>5</sup> that for room temperature low-energy boron implantations, the defect distribution extends to depths greater than the ion range (in contradiction with theoretical predictions) and anneal out at higher and higher temperatures as the implanted dose increases<sup>7</sup>. However, the boron ion, which is light, produces damage which is annealed at 900-1100°C.

**Dose:** The required dose is determined by the sheet resistance of the implanted layer. Fig. 5 shows that for 15 keV implantations, the sheet resistance becomes as small as  $20 \Omega/\square$  for a  $10^{16} \text{ cm}^{-2}$  dose followed by an 1100°C annealing. A 7 keV implantation needs a dose about ten times higher to give the same layer conductivity<sup>6</sup>.

**Experimental conditions.** To prepare the rectifying contact on N-type silicon, we implanted  $^{11}\text{B}^+$  ions of 10-15 keV energy at doses up to  $10^{16} \text{ cm}^{-2}$  and annealed the damage at 900-1000°C. The implantations were performed with an accelerator in our laboratory.

#### GLOW DISCHARGE

As the implantation just described is a rather sophisticated technique which needs expensive equipment, we developed a glow discharge procedure for fabricating heavily doped layers quickly, simply and at low cost.

**Principle.** The apparatus is shown schematically in fig. 6. The device upon which the contact is to be formed is used as a cathode inside a pyrex chamber which is first evacuated and then filled with  $\text{BF}_3$  to pressures of 0.01 to 0.1 torr. (For phosphorous doping, gaseous compounds like  $\text{PF}_3$  can be used). With a d.c. voltage applied through a 1 M $\Omega$  resistor, the discharge current on the order of a few milli-ampères flows. In order to avoid contamination, the anode is made of silicon. This simple system could easily be adapted to a cheap on-line production system which can be coupled for example, with a ribbon growing process. By a proper choice of the d.c. voltage, the sample can be either cleaned by sputtering off the surface atoms of the cathode (below 4 kV), or doped with boron (5-10 kV). Generally speaking, a heavily doped layer is obtained simply and quickly. In contrast to the  $^{11}\text{B}^+$  ion implantation, no mass separation of the ionized gas is performed. For a  $\text{BF}_3$  discharge, not only boron atoms are implanted in the target, but also heavy ionized fragments like  $\text{BF}_3^+$ ,  $\text{BF}_2^+$ , ... (these latter being at a concentration 5-10 times higher than that of the boron ions in the discharge). These low energy heavy ions, which have a very short range (about 0.2 of that of the boron ions of the same energy) produce a very thin but heavily damaged layer located close to the surface. Rutherford backscattering measurements have shown that the thickness of this layer before annealing is below the resolution of the experimental system (about 350  $\text{Å}$ ).

**Annealing.** The formation of an amorphous layer has an interesting consequence on the annealing temperature of the bombarded samples. It is well known that the electrical activity of implanted boron ions increases much faster with temperature when an amorphous structure is reached during implantation. An amorphous structure is not achieved for room temperature boron implantation but can be attained either by low temperature bombardment<sup>8</sup>, predamaging with inactive ions (Ne for example)<sup>9</sup> or  $\text{BF}_3^+$  or  $\text{BF}_2^+$  implants<sup>10</sup>. As shown in fig. 7, instead of an annealing temperature of 900-1000°C necessary to reach high electrical boron activity after the negative annealing stage, a temperature of 500-700°C is sufficient to reach full electrical activity. This temperature is well below general diffusion conditions.

**Bombarding time.** The experimental discharge conditions (current and time) have been determined by measuring the sheet resistance of the layer as a function of the current-time product, which is equivalent to an implanted dose. As shown in fig. 8, a value of  $32 \Omega/\square$  is reached in less than 5 minutes for a  $2 \text{ mA/cm}^2$  discharge current density. The same value of the sheet resistance is obtained with a  $10^{16} \text{ cm}^{-2}$ , 15 keV boron implantation followed by an 1100°C annealing.

Until now, only a few experiments have been done using  $\text{PF}_5$  gas to produce the back contact (ohmic contact) on N-type samples contacted on the front side with a  $\text{BF}_3$  discharge. Quite identical results for  $\text{BF}_3$  and  $\text{PF}_5$  have been obtained and it may be expected that this double discharge process can be used to produce solar cells either on N or P-type silicon at temperatures much lower than that used in diffusion processes.

#### PREBOMBARDED SCHOTTKY BARRIERS

The use of silicon Schottky barriers for solar cells was proposed several years ago<sup>11</sup>, but, in spite of the simplicity of this technique, not much work was devoted to it until recently. This was probably because of the low open circuit voltage and efficiency reached by these devices when compared to diffused cells. Recent work of ANDERSON<sup>2,3</sup> and PUL-FREY<sup>12</sup> stimulated interest in this procedure. As already indicated in fig. 2 and first calculated by PUL-FREY<sup>12</sup> the efficiency of an ideal Schottky solar cell strongly depends upon the barrier height  $\phi_{\text{B}}$  at the metal-semiconductor interface. It can be shown that the efficiency  $\eta$  in silicon at 300°K is related to  $\phi_{\text{B}}$  by  $\eta(\%) = 41.2 \phi_{\text{B}}(\text{eV}) - 22.7$ , for ideal AMO conditions without reflection losses and unity quantum yield and collection efficiency. As the conventional barrier height, for enough gold on N-type silicon, is about 0.8 eV, it results that the efficiency of these cells cannot exceed about 10%. An increase of  $\phi_{\text{B}}$  up to 1 eV will lead to a calculated efficiency of about 18%. Such an increase can be obtained either by a helium contact<sup>13-14</sup> or by a proper change of the band bending at the contact. The latter can be produced by doping a shallow layer close to the surface with ions so as to give a space charge whose type is opposite to that of the substrate. The band diagram of a Schottky barrier on N-type material with a net doping density  $[N_{\text{D}} - N_{\text{A}}]$  is shown in fig. 9a. If an interfacial layer with thickness  $X$  and acceptor concentration  $N$  has been produced by implantation, the band diagram is modified as shown in fig. 9b without any change of barrier height as long as the introduced doping dose  $D = NX$  is maintained below a critical value  $D_0$  expressed by

$$D_0 = r \frac{2eV_0}{e} (N_D - N_A)^{1/2},$$

where  $V_0$  is the contact potential of the conventional Schottky barrier and the other symbols have their usual meanings. When  $D$  becomes larger than  $D_0$  the barrier height  $\phi_{Bn}$  increases to a value  $\phi_{Bn}^*$  as shown in fig. 9c, which depends upon the dose  $D$ . As long as the interfacial layer remains fully depleted without external bias applied,  $\phi_{Bn}^*$  increases with dose. When  $D$  reaches a maximum value  $D_{max}$  such that the Fermi level is close to the valence band, the shallow layer is no longer fully depleted and a classical implanted P-N junction is formed. The situation resulting from the bombardment of a P-type substrate by N-type ions has been described by SHANNON<sup>15</sup>. For an N-type  $10 \Omega\text{-cm}$  substrate, the critical dose  $D_0$  is about  $10^{11} - 10^{12} \text{ cm}^{-2}$ . Consequently, precise knowledge of dose  $D$  and thickness  $X$  is necessary. These parameters are well known in the case of ion implantation. Using antimony ions implanted in a P-type substrate, SHANNON<sup>15</sup> has shown that it is possible to increase the barrier of a nickel Schottky diode from 0.49 to 0.78 eV. In order to reach a higher  $\phi_{Bn}$  value, we investigated gold Schottky barriers made on N-type silicon bombarded previously with 30 keV gallium or 5 keV boron ions, for which the range is about  $220 \text{ \AA}$ . Doses ranging from  $10^{11}$  to  $10^{13} \text{ cm}^{-2}$  were used and annealing was performed in vacuum at  $400^\circ\text{C}$  for the gallium and at  $800^\circ\text{C}$  for the boron implants. Fig. 10 shows the behaviour of  $\phi_{Bn}^*$  as determined by capacitance measurements as a function of boron and gallium implanted doses. A barrier height close to 1 eV is reached after  $10^{12} \text{ cm}^{-2}$  boron or  $10^{13} \text{ cm}^{-2}$  gallium implantations. The implanted samples gave  $\phi_{Bn}^* = 0.78 \text{ eV}$  for the gold-N-type silicon contact, in good agreement with the value found in the literature<sup>16-18</sup>. The variation of the dose with the nature of the ion arose from the different electrical activities: after a  $400^\circ\text{C}$  annealing the electrical activity of the implanted gallium layer is about ten times less than that of the same dose of boron implanted ions followed by a  $800^\circ\text{C}$  annealing. It should be noticed that a change of diode capacity with the frequency of the bridge is observed, indicating that even after annealing deep trapping levels are present. Since the damage for heavier ions is more important than that resulting from boron bombardment, the frequency dependence of the capacity is more important for the gallium implants.

#### APPLICATION TO SOLAR CELLS

**Device preparation.** The above described techniques were applied to prepare solar cells. As our purpose was mainly to demonstrate the usefulness of new techniques, only preliminary results will be given here.

N-type silicon with resistivities ranging from 0.5 to  $150 \Omega\text{-cm}$  was used to perform the experiments. After ion bombardment either by implantation or glow discharge, the samples were annealed 30 minutes under vacuum. Then either gold or silver grids were deposited by evaporation on the rectifying layer. In the case of Schottky barriers, no grids were used and a  $100 \text{ \AA}$  gold film was deposited. The back contacts for these diodes were generally made by an aluminium evaporation. Since this leads to rather high series resistances, a PF<sub>3</sub> glow discharge was used on some samples. An antireflecting coating consisting of  $600 \text{ \AA}$  of SiO<sub>2</sub> was sometimes deposited on the samples.

**Spectral response.** The spectral responses, normalized to  $100 \%$  at  $5500 \text{ \AA}$  wavelength, of typical cells in the short wavelength range are shown in fig. 11. In all cases they compare favorably with a commercial diffused cell (curve 1). The response of a BF<sub>3</sub> discharge contact (curve 2) is quite the same as that of a  $15 \text{ keV}$  ( $10^{13} \text{ cm}^{-2}$ ) implanted structure (curve 3). The best results were obtained with Schottky barriers and we found that the implantation of a low dose ( $10^{12} \text{ cm}^{-2}$ ) of boron ions does not change the spectral response very much (curve 5). It appears that a noticeable short wavelength efficiency improvement is obtained in these latter case, when compared to the diffused cell.

**Open circuit voltage.** The open circuit voltage  $V_{oc}$  of the devices was measured under a tungsten lamp illumination of  $100 \text{ mW/cm}^2$ . Under our experimental conditions the  $V_{oc}$  value of the diffused commercial cell was  $550 \text{ mV}$ .

The results for boron implantations for various doses are reported in table III.

TABLE III

Open circuit voltage for boron implanted diodes (mV)

Dose ( $\text{cm}^{-2}$ )		10 <sup>13</sup>	10 <sup>14</sup>	5.10 <sup>14</sup>	10 <sup>15</sup>	10 <sup>16</sup>	10 <sup>17</sup>
		0.5 $\Omega\text{-cm}$	15 keV	430	470	520	530
	30 keV	410	480	490	500		
10 $\Omega\text{-cm}$	15 keV	500			570		
150 $\Omega\text{-cm}$	5 keV	305	370		390	415	430

As expected the highest voltages were reached in the lower resistivity material implanted at high doses. This confirms the necessity of high implantation doses. Taking into account the rather high series resistance in our devices it is expected that the  $V_{oc}$  is identical to that of a diffused cell.

On table IV are reported the  $V_{oc}$  voltages measured on the BF<sub>3</sub> bombarded  $10 \Omega\text{-cm}$  N-type silicon. The results depend on the conditions (time x current), that is the dose, but are at least as good as for the boron implanted cells.

TABLE IV

Open circuit voltage for glow discharge diodes

Discharge voltage (kV)	Time x $i$ (discharge current) (min. mA/cm <sup>2</sup> )	$V_{oc}$ (mV)
6	1, 1	500
7	1, 2	520
7	1, 9	515
10	2, 2	530

## FIGURE CAPTIONS

- Fig. 1 : Relative efficiency of silicon solar cells at 300°K in AMO conditions as a function of the dead layer.
- Fig. 2 : Absolute efficiency of silicon Schottky solar cells at 300°K, in AMO conditions, as a function of the barrier height at the metal-semiconductor contact.
- Fig. 3 : Relative electrical activity after annealing of boron and phosphorous in silicon as a function of implantation energy.
- Fig. 4 : Plot of the dead layer due to boron implanted in silicon as a function of ion energy for various doping levels of the substrate. The projected range  $R_p$  of boron is also shown.
- Fig. 5 : Behaviour of sheet resistance for boron implanted silicon as a function of doses. Shaded curve is from ref. 6.
- Fig. 6 : Schematic view of the glow discharge apparatus.
- Fig. 7 : Relative electrical activity of boron and  $BF_3$  implanted layers as a function of annealing temperature in silicon.
- Fig. 8 : Sheet resistance for glow discharge contacts as a function of experimental conditions.
- Fig. 9 : Band diagram of a Schottky N-type silicon bombarded barrier: a) conventional; b) implanted dose  $D < D_0$  results in no  $\phi_{Bn}$  increase; c) implanted dose  $D > D_0$  giving a higher effective barrier height  $\phi_{Bn}$ .
- Fig. 10 : Increase of the barrier height  $\phi_{Bn}$  of gold Schottky barriers implanted respectively with boron and gallium.
- Fig. 11 : Spectral response at short wavelengths of various cells. The spectral response has been normalized to 100 % at 5500 Å.

TABLE VI

SHORT CIRCUIT CURRENT

Front contact	Boron implantation			BF <sub>3</sub> discharge	Schottky im- planted barrier 10 <sup>12</sup> cm <sup>-2</sup> boron
	10 <sup>14</sup> cm <sup>-2</sup>	5.10 <sup>14</sup> cm <sup>-2</sup>	10 <sup>15</sup> cm <sup>-2</sup>		
Back cont act	aluminium	alloyed	aluminium	PF <sub>5</sub> discharge	aluminium
I(mA/cm <sup>2</sup> )	9	16	13.5	22	8

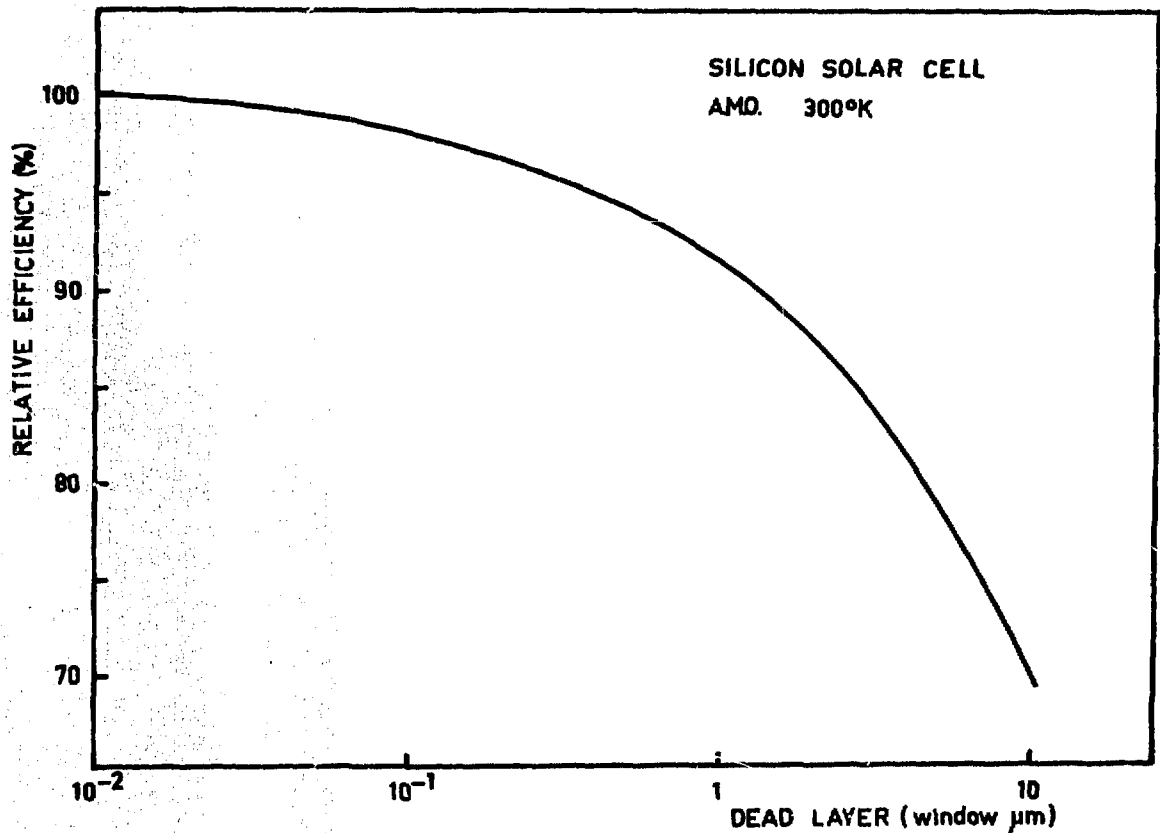


Fig. 1

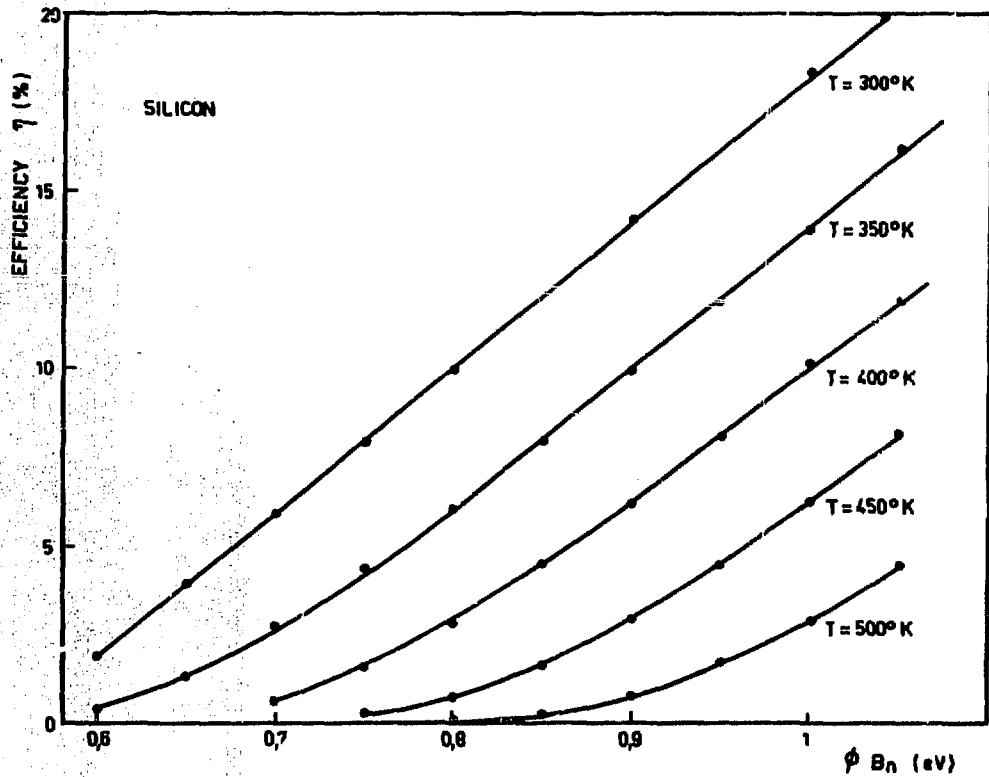


Fig. 2

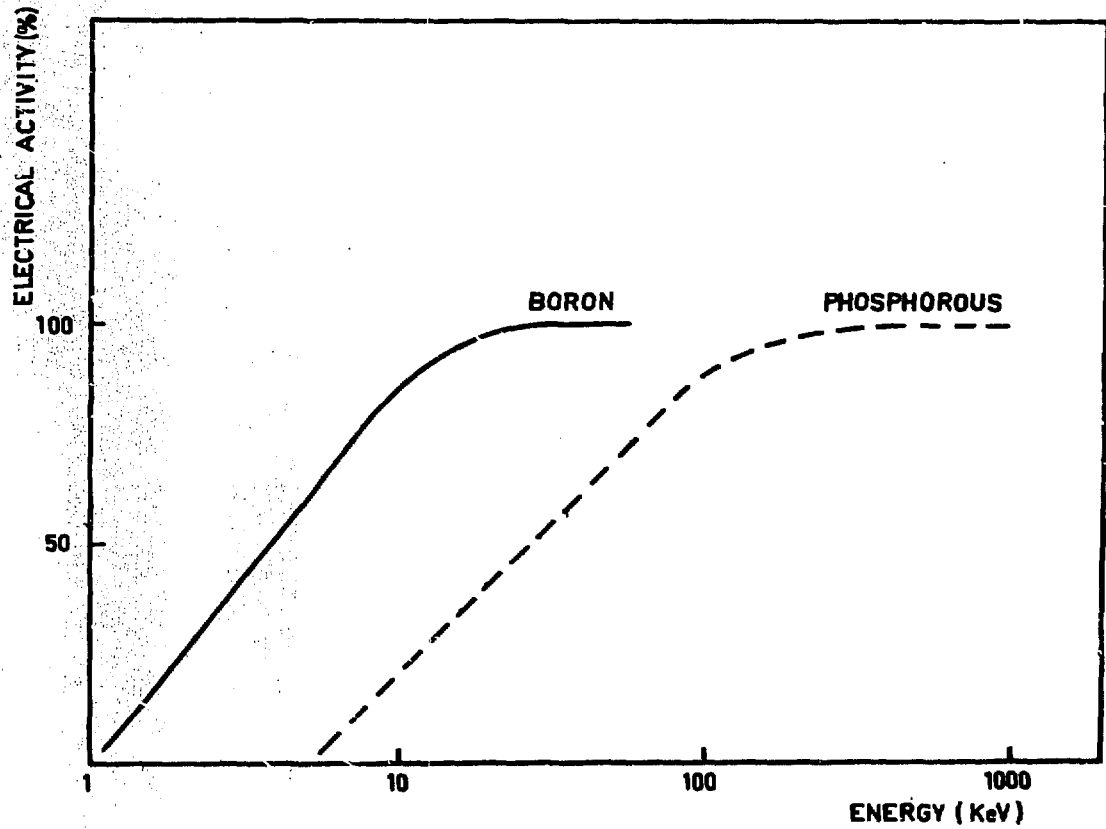


Fig. 3



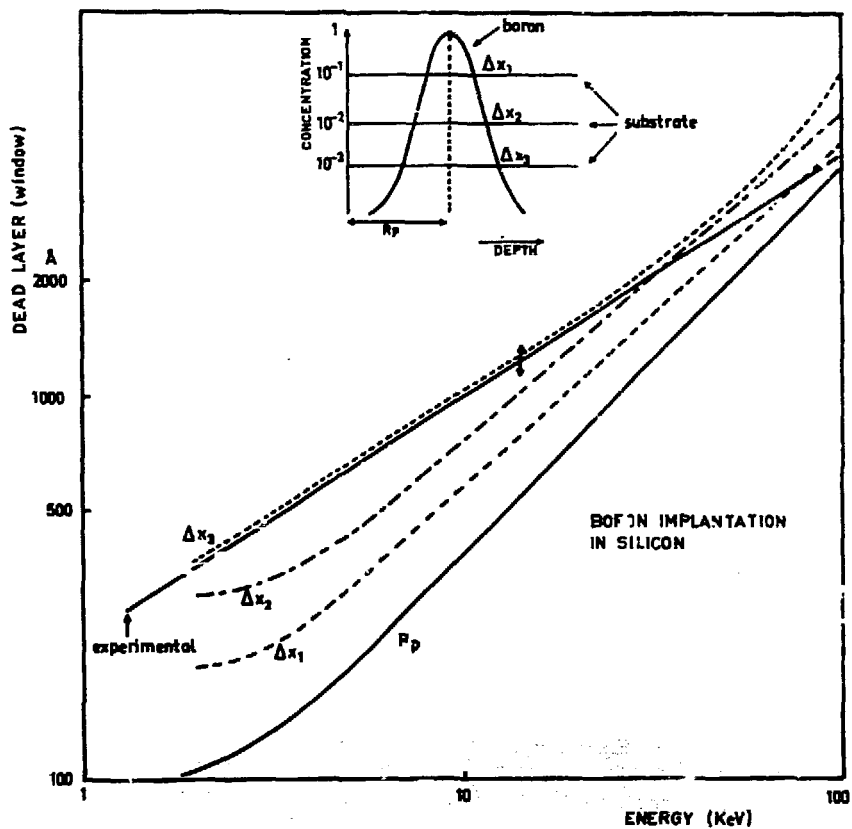


Fig. 4

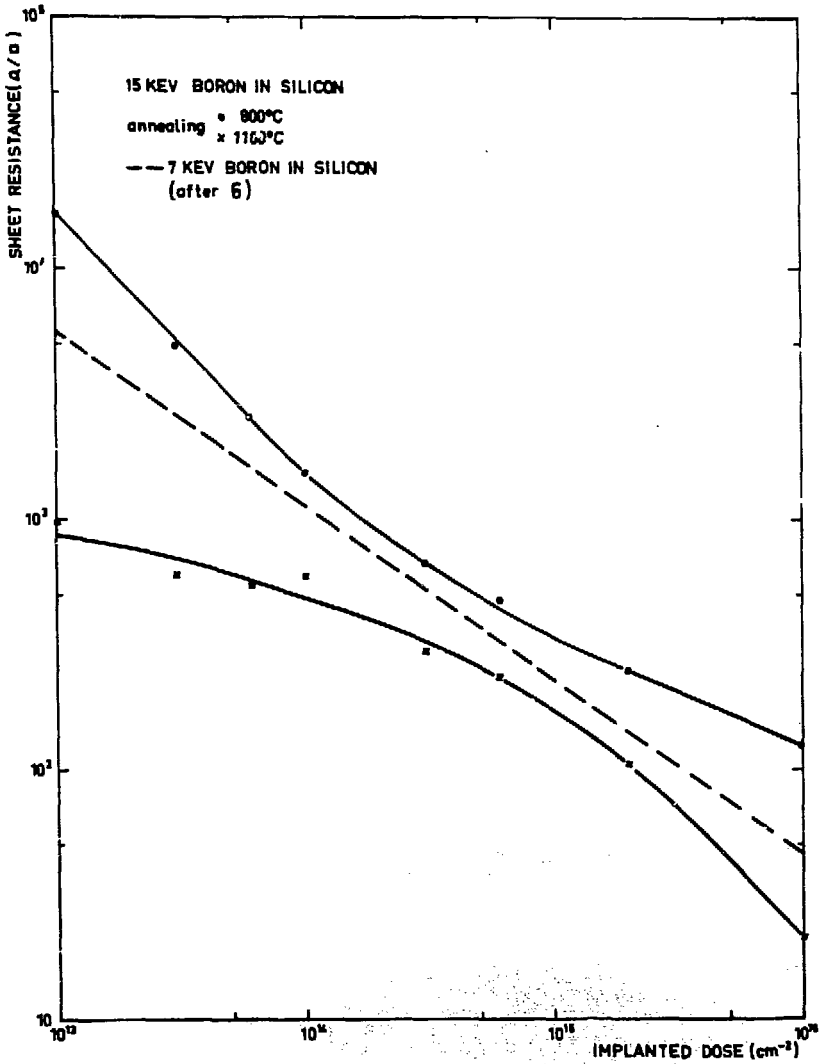


Fig. 5

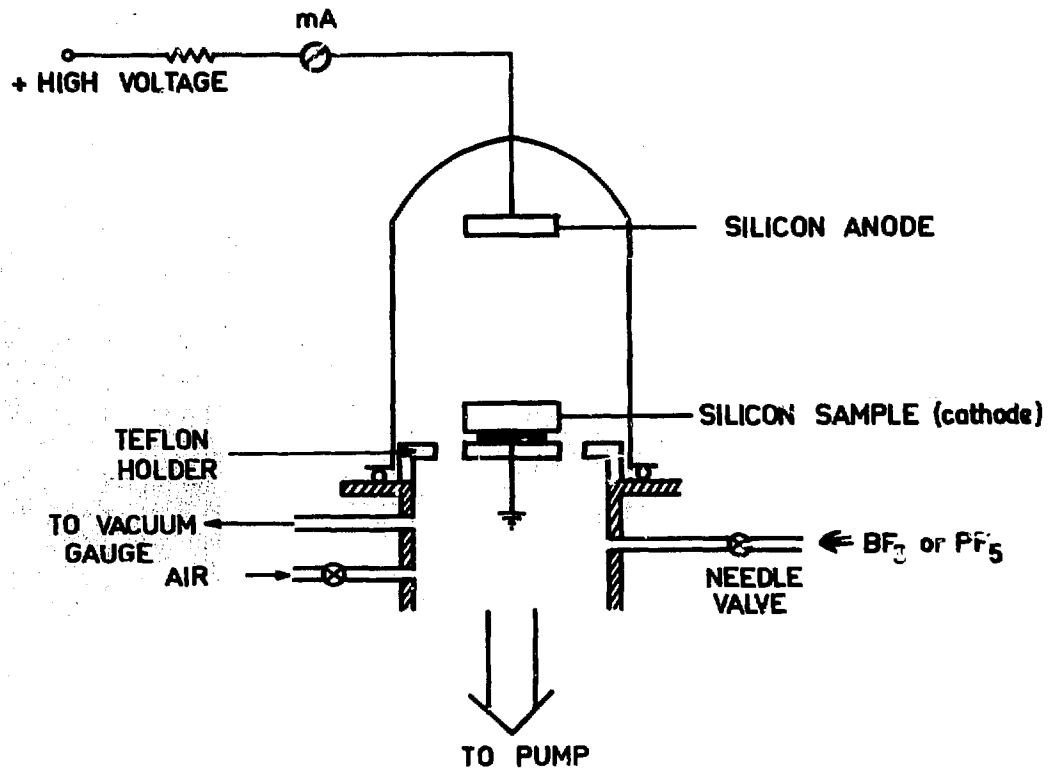


Fig. 6

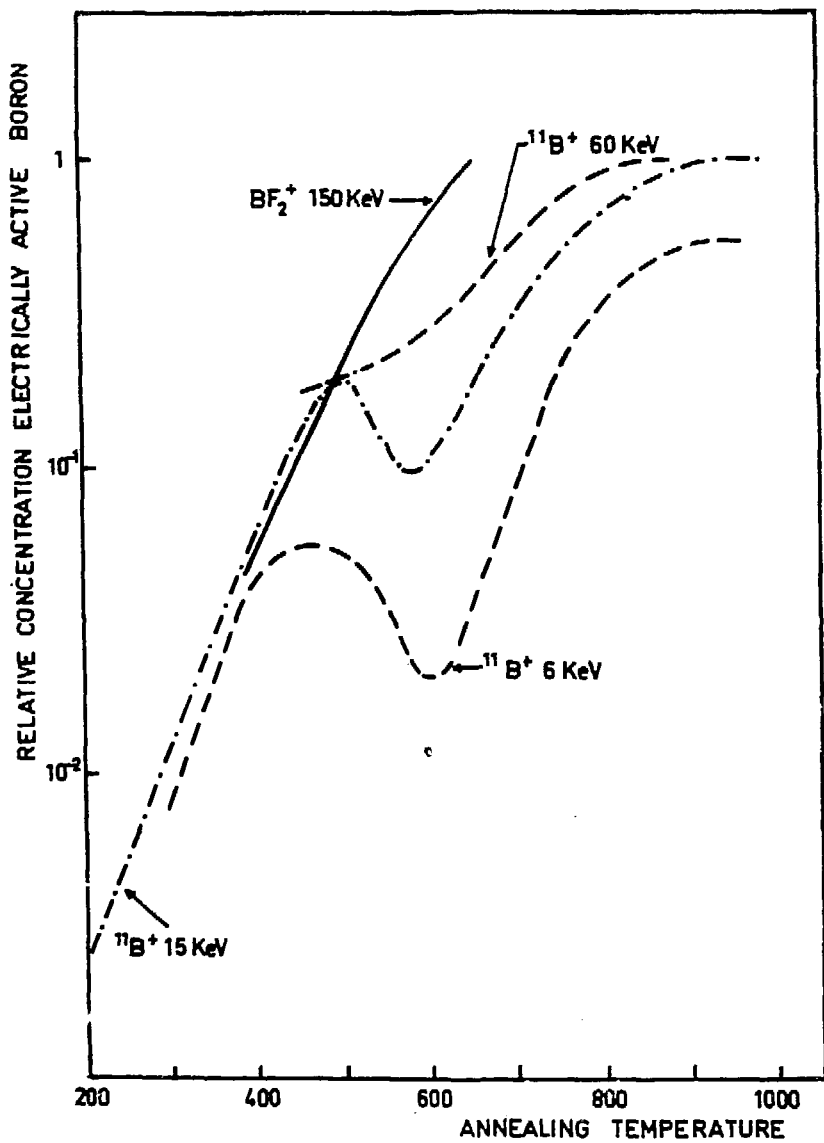


Fig. 7

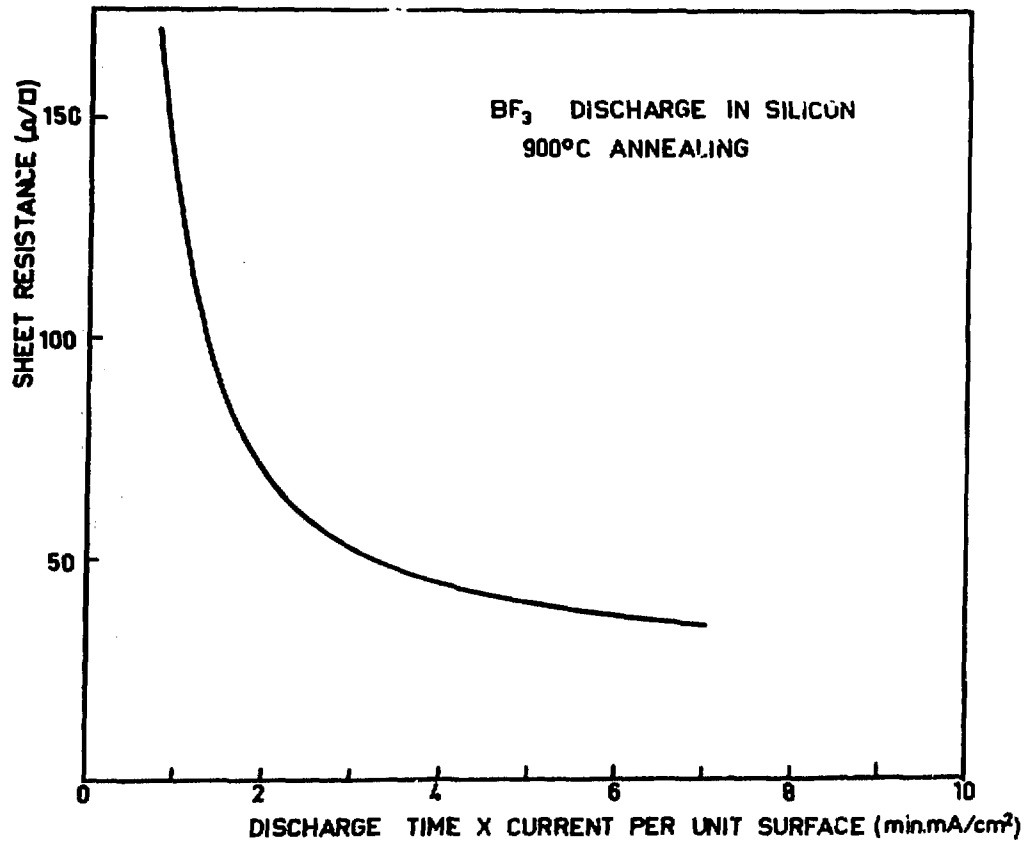
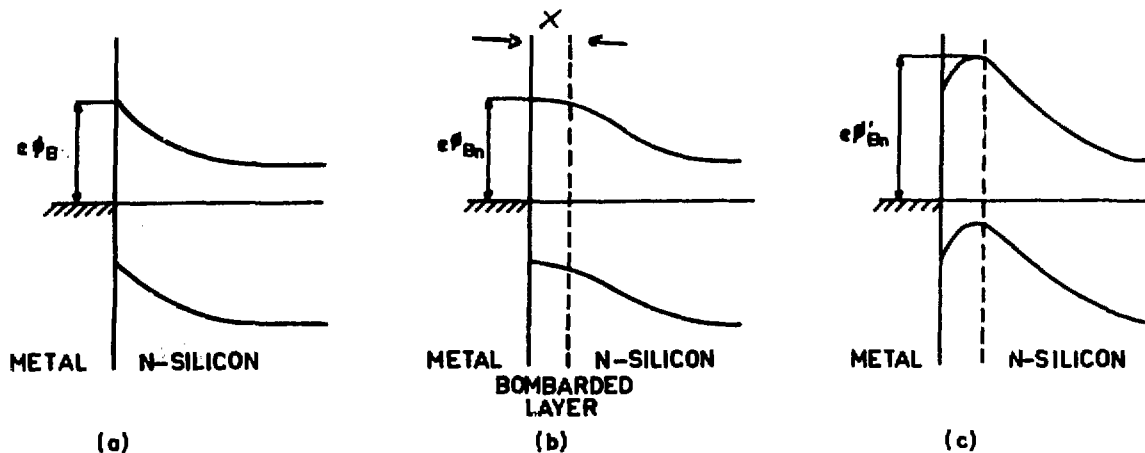


Fig. 8

BAND DIAGRAM OF A SCHOTTKY BARRIER WITH AN INTERFACIAL IMPLANTED LAYER



(a) NO IMPLANTED LAYER (conventional barrier)

(b) IMPLANTED DOSE  $D < D_{min}$

(c)  $D_{min} < D < D_{max}$

Fig. 9

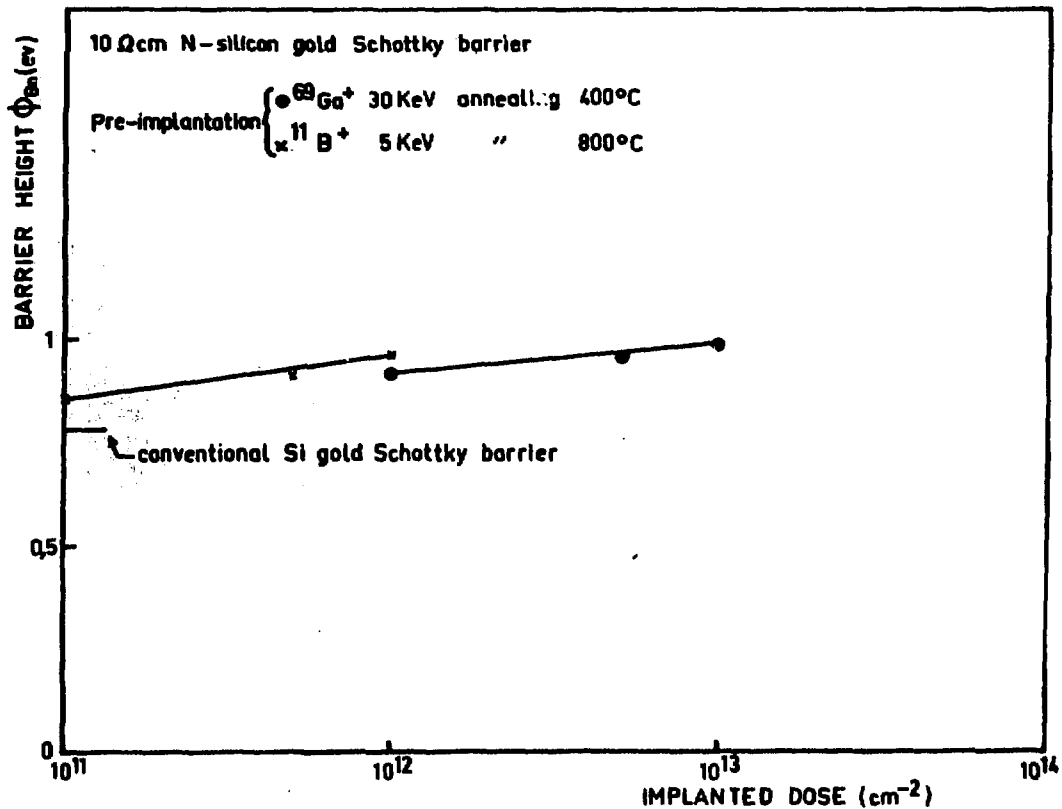


Fig.10

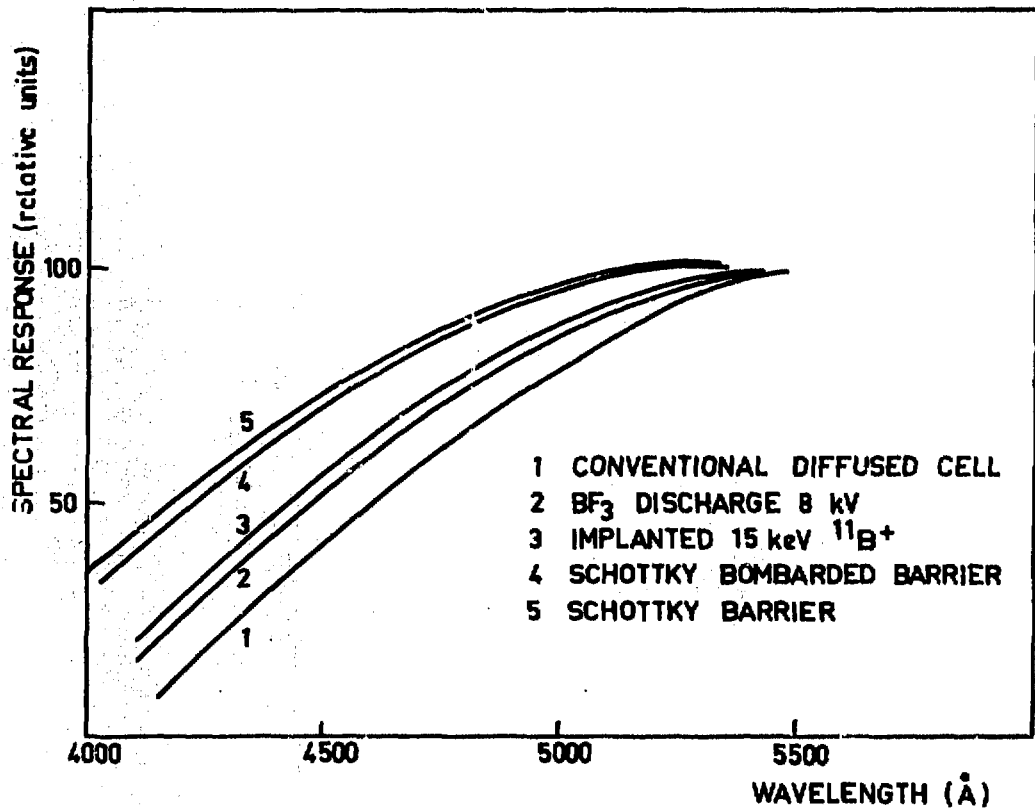


Fig. 11